Science in China Series D: Earth Sciences

Geochemistry and Sr-Nd isotope characteristics of tonalites in Zêtang, Tibet: New evidence for intra-Tethyan subduction

WEI DongLiang[1,2], XIA Bin[1†], ZHOU GuoQing[1,3], YAN Jun[1], WANG Ran[1,2] & ZHONG LiFeng[1,2]

[1] Key Laboratory of Marginal Sea Geology, Guangzhou Institute of Geochemistry, Chinese Academy of Sciences, Guangzhou 510640, China;
[2] Graduate University of Chinese Academy of Sciences, Beijing 100049, China;
[3] Department of Earth Sciences, Nanjing University, Nanjing 210093, China

Tonalites from the island arc rock assemblage in the Zêtang segment of the Yarlung Zangbo suture zone were analyzed for major, trace elements (including REE) and Sr-Nd isotope. The experimental data demonstrate that the tonalites have the adakite-like characteristics, including high SiO_2 (58%—63%), Al_2O_3 (18.4%—22.4%), Sr (810×10^{-6}—940×10^{-6}), Sr/Y (77—106), low HREE (Y=9×10^{-6}—11×10^{-6}, Yb=1×10^{-6}—1.3×10^{-6}), with LREE enrichment and faint Eu positive anomaly. I_{Sr} (0.70421—0.70487) is relatively low whereas $^{143}Nd/^{144}Nd$ (0.512896—0.512929) and $\varepsilon_{Nd}(t)$ values (+6.7—+7.3) are high. These features suggest that Zêtang tonalites were formed by the partial melting of subducted oceanic crust, with involvement of a small amount of oceanic sediments. The identification of Zêtang adakites, derived from slab melting, presents new evidence for the intra-Tethyan subduction and the previous suggestion about the existence of intra-oceanic island arc within Tethys.

adakite, Zêtang tonalites, subduction, Yarlung Zangbo suture zone, Tibet

Adakite (adakite-like rock) is a type of igneous rock with remarkable geochemical characteristics: high SiO_2 (>56%), Al_2O_3 (>15%), Sr (>400×10^{-6}), Sr/Y(>20—40), La/Yb>20, enriched in Na_2O ($Na_2O>K_2O$) and LREE, but depleted in Y and HREE (Y<18×10^{-6}, Yb<1.9×10^{-6}). It is a traditional view that adakite is derived from the partial melting of young and hot subducted oceanic crust at a depth about 75—85 km (corresponding to amphibolite-eclogite transition zone)[1]. Recent studies show that the melting of underplated basalt and delaminated lower crust can also produce the adakite (adakite-like rock)[2−5]. Whichever genesis it is, adakite (adakite-like rock) records the deep dynamic process of plate movement (such as slab subducting, basalt underplating, delamination of lower crust) and it is of high importance in geodynamics.

The Tibetan Plateau is the result of Tethyan subduction, extinction and Indian-Asian continent collision, and has attracted extensive attention of geologists all over the world. Zhang et al.[6] first suggested the development of Cenozoic adakites on the Tibetan Plateau. In addition, some researchers have identified adakites in northern Tibet and proposed that these rocks were generated by the partial melting of thickened lower crust, recording the thickening event of the Tibetan Plateau[7−11]. The intrusive rocks within the Miocene Gangdese Cu-bearing porphyry belt in southern Tibet also exhibit a geochemical affinity with adakite. The genesis

Received May 8, 2006; accepted July 17, 2006
doi: 10.1007/s11430-007-0034-8
†Corresponding author (email: xiabin@gig.ac.cn)
Supported by the National Natural Science Key Foundation of China (Grant No. 40534019), Open Research Fund Program of Key Laboratory of Marginal Sea Geology of the Chinese Academy of Sciences (Grant No. MSGL-04-13) and the Knowledge Innovation Program of the Chinese Academy of Sciences (Grant No. KZCXZ-SW-117)

of these rocks is ambiguous[12] despite the suggestion that they were produced by the melting of the thickened Gangdese lower crust[13−16].

However, no adakites have been reported in the Yarlung Zangbo suture zone as yet. In this study, the adakites in the Zêtang segment of the Yarlung Zangbo suture zone were discovered and identified for the first time. This discovery provides important evidence for the formation and evolution of the suture zone in the Zêtang area and the Tethyan tectonic reconstruction.

1 Geological setting and petrology

The research area is located near Zêtang Town in southern Tibet and belongs to the eastern segment of the Yarlung Zangbo suture zone, composed of a suit of island arc rock assemblage and ophiolite. To the south, there are Triassic flysch deposits (Jiedexiu Group, T_3j, including slate, sandstone and limestone lenses), representing the passive continent marginal sediments of the northern Indian plate. To the north, separated by the Yarlung Zangbo River fault belt, the Late Jurassic and Early Cretaceous volcanic sedimentary formations are developed.

Zêtang ophiolite extends almost 20 km in east-west (~45 km^2)[17,18] (Figure 1), contacting with the north arc rocks assemblage by a fault. Although the ophiolite has undergone complicated tectonic movements, its sequence is basically completed, composed mainly of peridotite, cumulate complexes, diabase and gabbro dyke swarms and pillowed and massive basalts.

So far, there are still many debates on the formation environment of Zêtang ophiolite, such as island arc or marginal ocean, marginal ocean basin, etc.[19−21]. This hinders our further understanding about the tectonic evolution in the Zêtang segment of the Yarlung Zangbo suture zone. Aitchinson et al.[22,23] and McDermid et al.[24] named the arc rock assemblage in the north of Zêtang ophiolite as "Zêtang terrane", and suggested that this terrane may represent a intra-oceanic island arc within Tethys ocean in Mesozoic (161−152 Ma) and the south Zêtang ophiolite was formed in forearc environment. Previous studies revealed that Zêtang ophiolite was probably developed on the intra-oceanic subduction belt (SSZ-type), but lack of more evidence to prove the existence of this subduction belt. In this paper, the intra-Tethyan subdution event is discussed, based on the detailed research of adakitic tonalites identified from Zêtang island arc.

The Zêtang island arc rock assemblage crops out about 25 km^2 near Zêtang Town, 12 km long in east-west trends. Toward the north, the assemblage is overlain by the Quaternary sediments, and toward the south, it is fault contacted with Zêtang ophiolite. The components of this assemblage are very complicated: the igneous rocks include basaltic-rhyolitic extrusives and gabbroic-dioritic intrusives; volcaniclastics include

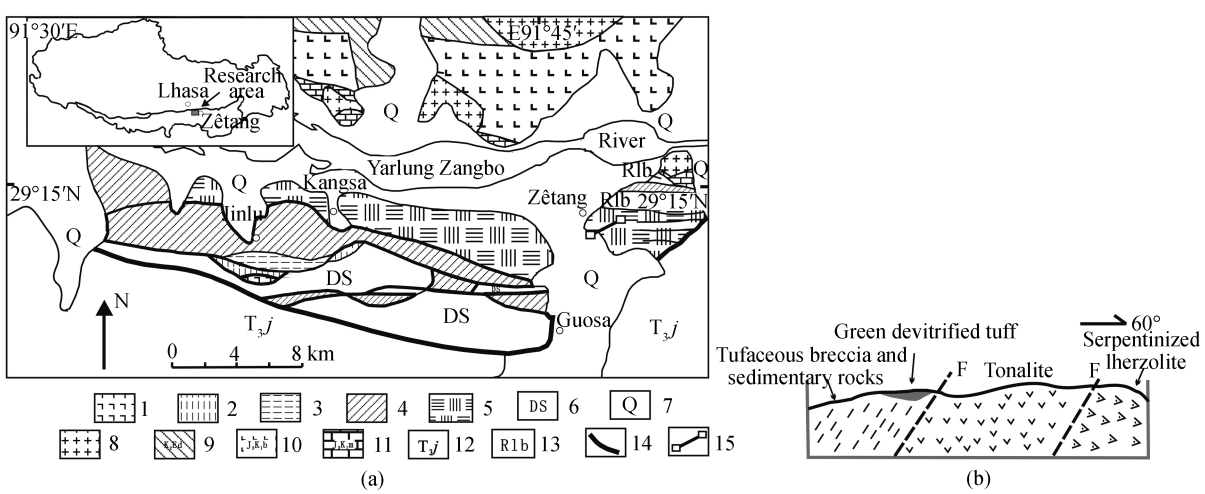

Figure 1 (a) Geological sketch map of Zêtang area (modified from 1:200000 geological map). 1, Pillowed and massive lavas; 2, dyke swarms (diabase and gabbro); 3, cumulative complex; 4, ultramafic rocks; 5, island arc igneous rock assemblage; 6, colorful flysch chert rocks; 7, quaternary; 8, granite; 9, Danshiting Group; 10, Bima Group; 11, Mamuxia Group; 12, Jiedexiu Group; 13, Luobusha Group; 14, fault; 15, samples section. (b) Sketch of samples section.

volcanic breccias, volcaniclastic sandstone, siltstone, mudstone, tuff with limestone blocks, and devitrified tuffs[25]. Lithologically, the adakites reported herein are tonalites which occurred as stocks. Their wall rocks include serpentinized lherzolite, amphibolite, breccia tuff, etc. The dominant minerals in Zêtang tonalites are plagioclase, hornblende, biotite and quartz. The accessory minerals are tourmaline, apatite and zoisite. The plagioclase is mostly prehnite-epidote bearing. The biotite has been altered to muscovite or muscovite+epidote. The hornblende is plentiful and acicular, and the big hornblende phenocrysts have hidden bandings, yellowy in centre and bottle green in margin. The quartz is distributed unequally, mostly filling in the caves of biotite, hornblende and plagioclase, similar to the graphic structure.

2 Analytical methods and results

13 fresh rock samples were collected for major and trace elements analyses. The sample preparation and analyses were carried out at the Institute of Geochemistry, Chinese Academy of Sciences. Major elements were measured by the traditional wet chemical method and trace elements (including REE) were analyzed on the Inductively Coupled Plasma-Mass Spectrometev (ICP-MS)[26]. The sample preparation was performed as follows: 50 mg of powdered basalt sample was placed in a PTFE bomb. 1 mL of HF (38%) and 0.5 mL of HNO_3 (68%) were added to each sample. The bombs were then placed on a hot plate, and the solution evaporated to remove most of the silica. 1 mL of HF and 0.5 mL of HNO_3 were then added. The sealed bombs were placed in an electric oven and heated to 190℃ for 12 h. After cooling, the bombs were opened, 1 mL of 0.5 μg/mL Rh solution was added as an internal standard and placed on a hot plate (at ca. 150℃), and the solutions evaporated to dryness. 1 mL of HNO_3 was added, evaporated to dryness and followed by a second addition of HNO_3 and evaporation to dryness. The final residue was re-dissolved by adding 8 mL of 40% HNO_3, re-sealing the bombs and returning them to the electric oven heated at 110℃ for 3 h. After cooling, the final solution was made up to a 100 mL by addition of distilled de-ionized water.

On the basis of major and trace elements data, we selected 5 from the 13 samples to analyze the Sr-Nd isotopic composition. The Sr-Nd isotope was measured with a MAT262 (Finnigan, Germany) mass spectrometer in Institute of Geology and Geophysics, Chinese Academy of Sciences. The process follows the subsequent procedure[27,28]: ^{87}Rb-^{84}Sr and ^{149}Sm-^{150}Nd mixed with diluter and HF-$HClO_4$ mixture was added into ~100 mg of whole-rock powder and then the sample was decomposed completely at high temperature. The separation and purification of Rb-Sr and REE were carried out on the quartz exchange columns with a 5 mL AG50W-X1 (200－400 mesh) exchange resin, whereas Nd was separated and purified with the Teflon powder as exchange medium. Sr isotopic ratios were measured using Ta filament and Ta-Hf emission reagent, and the Rb, Nd isotopic ratios were determined in a Re double-filament configuration. Nd and Sr isotopic ratios were normailized to $^{146}Nd/^{144}Nd=0.7219$ and $^{86}Sr/^{88}Sr=0.1194$, respectively. Total procedural blanks were ＜300 pg for Nd and ＜100 Pg for Sr (Table 1).

3 Geochemistry

3.1 Major elements

Zêtang tonalites are characterized by high SiO_2 (58%－63%), Al_2O_3 (18.4%－22.4%), Na_2O (3.2%－4.12%), Na_2O/K_2O (1.6－2.8), low MgO (0.69%－1.08%), TiO_2 (0.25%－0.3%), and significantly peraluminous (A/CNK = 0.98－1.35, A/NK=2.2－2.9). According to the CIPW normative mineral calculation results, we use the An-Ab-Or diagram (Figure 2) to classify the rocks. As shown in Figure 2, all samples are plotted within the "Tonalite" field (Table 2).

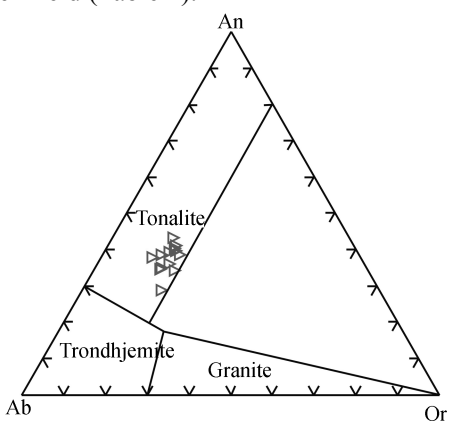

Figure 2 An-Ab-Or classification diagram[29].

3.2 Rare earth elements (REE)

All samples present fractionated REE patterns with

Table 1 Major (%) and rare earth elements ($\times10^{-6}$) data of Zêtang tonalites

Sample No.	ZD-130	ZD-131	ZD-132	ZD-133	ZD-135	ZD-136	ZD-137	ZD-138	ZD-139	ZD-140	ZD-141	ZD-142	ZD-143
SiO_2	63.69	63.18	61.66	60.53	60.95	59.40	61.37	63.01	57.98	62.14	62.26	63.09	60.32
TiO_2	0.28	0.27	0.26	0.27	0.29	0.28	0.27	0.25	0.26	0.25	0.30	0.29	0.28
Al_2O_3	18.71	19.55	21.07	20.86	20.55	22.39	21.16	20.47	21.78	21.70	18.40	18.71	19.94
Fe_2O_3	1.88	2.56	1.56	1.59	1.95	2.00	1.23	1.58	1.36	1.50	2.03	1.31	1.31
FeO	1.50	1.30	1.50	1.35	1.40	1.15	1.50	1.10	1.30	1.15	1.24	1.40	1.10
MnO	0.11	0.11	0.10	0.11	0.12	0.11	0.11	0.10	0.11	0.10	0.11	0.12	0.11
MgO	0.96	0.90	0.69	0.88	0.98	1.07	0.95	0.89	0.86	0.91	1.08	1.00	0.93
CaO	5.23	3.99	6.12	5.73	5.20	4.75	5.63	4.72	5.59	4.45	5.69	5.42	5.02
Na_2O	3.20	3.86	3.39	3.31	3.23	3.71	3.34	3.43	3.42	3.30	4.12	3.68	3.96
K_2O	1.99	2.01	1.70	1.83	1.64	1.72	1.81	1.82	1.95	1.98	1.48	1.58	1.86
P_2O_5	0.25	0.30	0.16	0.20	0.30	0.28	0.27	0.18	0.19	0.27	0.32	0.27	0.20
LOI	2.00	1.50	1.61	2.77	3.05	2.58	2.03	1.94	4.35	1.70	2.40	2.50	4.31
Total	99.86	99.63	99.82	99.48	99.78	99.55	99.68	99.58	99.32	99.41	99.53	99.43	99.47
Na_2O/K_2O	1.6	1.9	2.0	1.8	2.0	2.2	1.8	1.9	1.8	1.7	2.8	2.3	2.1
La	15.73	13.68	15.69	15.23	16.08	15.97	21.65	14.77	15.16	13.54	14.26	15.62	14.02
Ce	24.56	21.24	22.62	23.49	25.08	24.59	32.73	22.80	23.46	20.68	22.37	24.09	22.07
Pr	2.59	2.26	2.48	2.36	2.61	2.55	3.21	2.39	2.49	2.23	2.36	2.54	2.33
Nd	9.42	8.50	8.99	8.41	9.76	9.61	11.21	8.84	9.20	8.43	9.31	9.19	8.55
Sm	1.86	1.57	1.69	1.78	1.94	1.89	1.91	1.70	1.82	1.75	1.85	1.92	1.81
Eu	0.68	0.69	0.66	0.64	0.66	0.70	0.67	0.63	0.66	0.68	0.65	0.61	0.61
Gd	1.63	1.60	1.58	1.44	1.80	1.76	1.68	1.47	1.63	1.47	1.67	1.67	1.51
Tb	0.25	0.25	0.27	0.24	0.29	0.28	0.27	0.24	0.26	0.24	0.30	0.26	0.25
Dy	1.51	1.53	1.51	1.40	1.65	1.69	1.60	1.44	1.44	1.39	1.71	1.58	1.51
Ho	0.32	0.31	0.30	0.30	0.36	0.35	0.33	0.30	0.32	0.28	0.36	0.33	0.32
Er	0.96	0.87	0.91	0.92	0.98	1.10	1.01	0.86	0.90	0.92	1.08	1.04	1.02
Tm	0.14	0.15	0.14	0.14	0.18	0.15	0.16	0.13	0.16	0.14	0.18	0.16	0.16
Yb	1.17	1.05	1.03	1.11	1.27	1.28	1.19	1.00	1.08	1.02	1.28	1.23	1.22
Lu	0.18	0.17	0.18	0.18	0.21	0.21	0.18	0.17	0.21	0.17	0.20	0.20	0.19
La/Yb	13.45	12.98	15.22	13.75	12.71	12.47	18.16	14.71	14.05	13.3	11.12	12.68	11.53
∑REE	61.00	53.87	58.05	57.64	62.87	62.11	77.78	56.74	58.79	52.94	57.58	60.44	55.57

LREE-enrichment and faint Eu positive anomaly, δEu=+1.1—+1.3 (Figure 3). La/Yb ratios range in 11—15, slightly lower than the typical adakites; HREE are strongly depleted (Y=9×10^{-6}—11×10^{-6}, Yb=1×10^{-6}—1.3×10^{-6}), similar to that of the modern typical adakites (Y<18×10^{-6}, Yb<1.9×10^{-6}). It is remarkable for the strong depletion in MREE. $(Ho/Yb)_N$=0.77—0.86 indicates that MREE are more depleted than HREE (such as Yb, Lu).

3.3 Trace elements

As the trace elements spidergram shows (Figure 4), all samples display a uniform and right-dipping pattern, similar to those of the Costa Rica and Northern Xinjiang adakites[30,31], but more enriched in LILE (Cs, Rb, Ba) than that of the Xiwan albite granites[32]. Zêtang tonalites have obvious Th, Sr, P positive anomalies and Nb, Ta, Ti negative anomalies. This implies that the Ti-minerals (rutile) or amphibole was stable in residue, showing similar features to the island arc igneous rocks. The relatively low Y content suggests possible residues including amphibole, garnet and pyroxene. The characteristics of high Sr and low Y (Sr=810×10^{-6}—940×10^{-6}, Sr/Y=77—106) are coincident with the typical adakites (Sr>400×10^{-6}, Sr/Y>20—40), indicating that the plagioclase has entered the melt and there was no plagioclase in residue. In the Sr/Y-Y (Figure 5) and $(La/Yb)_N$-Yb_N diagrams (Figure 6), all the samples fall into the "Adakite" field.

3.4 Sr-Nd isotope

Five tonalite samples exhibit high and uniform $^{143}Nd/^{144}Nd$ (0.512896—0.512929) and $\varepsilon_{Nd}(t)$ values (+6.7—+7.3). $^{87}Sr/^{86}Sr$ values range between 0.704765—0.705020 and I_{Sr} between 0.70421—0.70488. These isotopic characteristics indicate that Zêtang tonalites should be derived from DM or the oceanic crust with DM characteristics rather than a continental

Table 2 Trace elements ($\times 10^{-6}$) and Sr-Nd isotopic compositions of Zêtang tonalites

Sample No.	ZD-130	ZD-131	ZD-132	ZD-133	ZD-135	ZD-136	ZD-137	ZD-138	ZD-139	ZD-140	ZD-141	ZD-142	ZD-143
Ba	1822.6	1841.5	1532.9	1512.2	848.28	809.88	1342	1517.8	1621.6	2049.3	1032.4	1051.2	1359
Rb	68.5	66.5	61.0	67.3	60.4	58.6	65.3	59.7	61.4	65.5	52.6	62.2	66.2
Sr	813.4	838.9	920.5	870.5	943.0	868.9	850.2	811.4	860.8	917.6	823.1	889.3	810.5
Cs	1.02	1.04	1.09	1.14	0.94	0.93	0.84	0.99	0.75	1.02	1.03	1.14	1.21
Li	5.0	5.9	3.0	6.1	8.0	6.4	5.9	5.5	8.7	4.6	10.2	4.6	8.3
Ga	16.8	17.0	17.5	16.6	17.5	16.5	17.0	16.5	16.8	16.8	16.7	17.3	17.7
Ta	0.18	0.15	0.14	0.16	0.24	0.22	0.17	0.16	0.16	0.16	0.25	0.21	0.22
Nb	3.35	3.23	2.96	3.26	3.36	3.37	3.30	3.04	3.28	3.06	3.29	3.71	3.62
Hf	2.28	2.12	1.99	2.44	2.09	2.35	2.33	2.14	2.41	2.14	2.14	2.37	2.40
Zr	79.16	73.53	71.44	88.35	73.21	81.56	81.65	74.83	83.71	75.31	75.26	80.39	79.92
Ti	1737.1	1677.2	1557.4	1677.2	1797	1737.1	1677.2	1557.4	1677.2	1557.4	1797	1797	1737.1
Y	9.24	8.98	9.22	8.94	10.43	10.93	9.87	8.67	9.26	8.60	10.69	10.34	9.42
Th	5.87	5.35	5.47	5.64	6.05	6.37	6.99	5.46	5.77	5.24	5.61	6.10	6.36
U	1.31	1.14	1.30	1.18	1.23	1.57	1.21	1.16	1.40	1.28	1.53	1.17	1.51
Cr	64.1	313.4	131.8	70.1	44.8	51.3	105.5	44.4	104.7	116.2	81.7	53.2	44.5
Ni	32.6	165.8	105.9	34.5	24.4	26.1	51.9	22.4	53.0	59.1	43.1	28.7	27.7
Co	5.7	7.0	6.1	5.3	6.1	6.1	5.8	5.5	5.5	6.0	6.7	5.9	5.9
Sc	5.1	5.1	5.1	4.5	4.5	5.5	5.1	3.7	4.8	3.8	5.5	4.5	5.1
V	66.8	65.2	69.5	64.9	74.7	74.1	65.1	63.9	64.5	63.9	79.9	67.1	64.7
Cu	6.4	17.3	39.1	6.1	8.8	13.1	6.6	7.5	4.2	6.5	7.3	6.7	11.0
Pb	21.3	22.9	23.0	26.0	23.9	22.5	24.1	22.6	24.5	21.6	21.6	21.2	24.7
Zn	40.4	43.9	33.2	48.9	55.0	41.8	43.6	37.3	39.6	46.6	44.1	41.9	43.7
Th/Ta	32.8	34.9	38.2	35.1	25.4	29.6	40.7	35.2	35.6	32.2	22.9	29.8	29.3
Sr/Y	88.1	93.5	99.9	97.4	90.4	79.5	86.2	93.7	93.0	106.7	77.0	86.0	86.0
$^{147}Sm/^{144}Nd$	0.1125	0.1146		0.1126	0.1204								0.1154
$^{143}Nd/^{144}Nd$	0.512929	0.512906		0.512896	0.512916								0.512910
2σ	0.000009	0.000012		0.000014	0.000015								0.000009
$\varepsilon_{Nd}(t)$	+7.3	+6.8		+6.7	+6.9								+6.9
$^{87}Rb/^{86}Sr$	0.067	0.231		0.231	0.216								0.255
$^{87}Sr/^{86}Sr$	0.705020	0.704970		0.704810	0.704787								0.704765
2σ	0.000018	0.000017		0.000020	0.000012								0.000011
I_{Sr}	0.70488	0.70447		0.70431	0.70432								0.70421

I_{Sr} and $\varepsilon_{Nd}(t)$ were calculated with t=152 Ma[24].

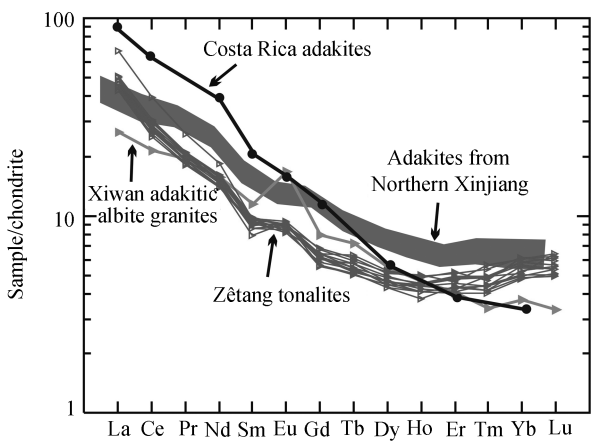

Figure 3 Chondrite-nomalized REE patterns.

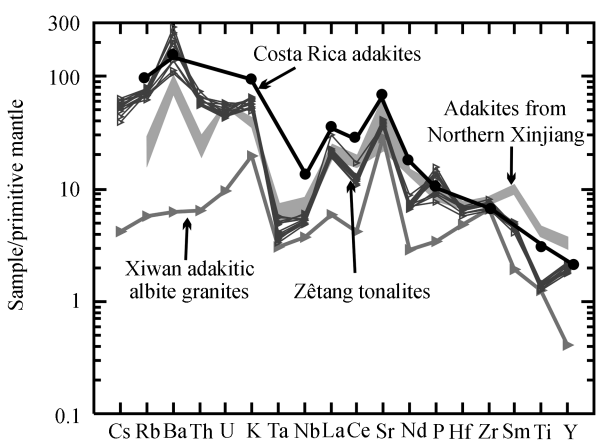

Figure 4 Primitive mantle-nomalized spidergram of trace elements.

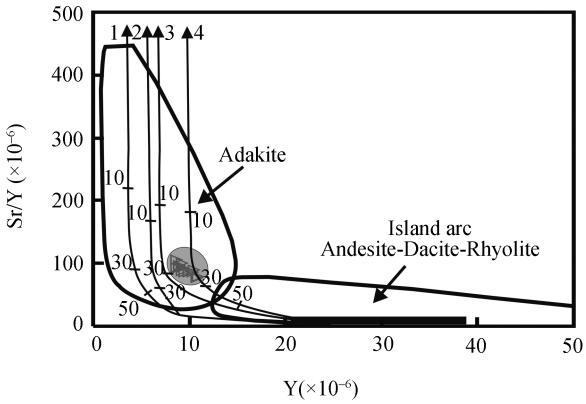

Figure 5 Sr/Y-Y diagram[1,33]. The curves represent various models of the partial melting of depleted and altered MORB with an amphibolite or eclogite residue. 1, Eclogite (gt/cpx =50/50); 2, amphibole garnetite (gt/am=50/50); 3, amphibole eclogite (am/gt/cpx=10/40/50); 4, garnet amphibolite (gt/am=10/90).

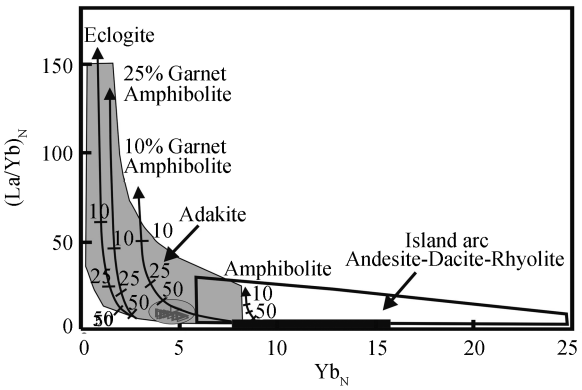

Figure 6 $(La/Yb)_N$-Yb_N diagram[33,34].

crust origin. The $\varepsilon_{Nd}(t)$ values are slightly lower and I_{Sr} are higher than those of MORB, suggesting the small volume involvement of oceanic sediments in the melting process.

The Sr-Nd isotopic compositions of Zêtang tonalites are far from those of the adakitic rocks in both East China and Cu-bearing porphyry belt of Gangdese arc. The former were produced by the partial melting of underplating basalt/delamination lower crust while the latter are thought to be generated by the partial melting of mafic materials in a thickened lower crust with input of enriched mantle and/or upper crust components[12,14]. The Sr-Nd isotopic compositions of all samples are close to the Yarlung Zangbo MORB and the adakites related to slab melting (Figure 7).

4 Discussion

4.1 Petrogenesis

Recent studies show that adakites can be produced in

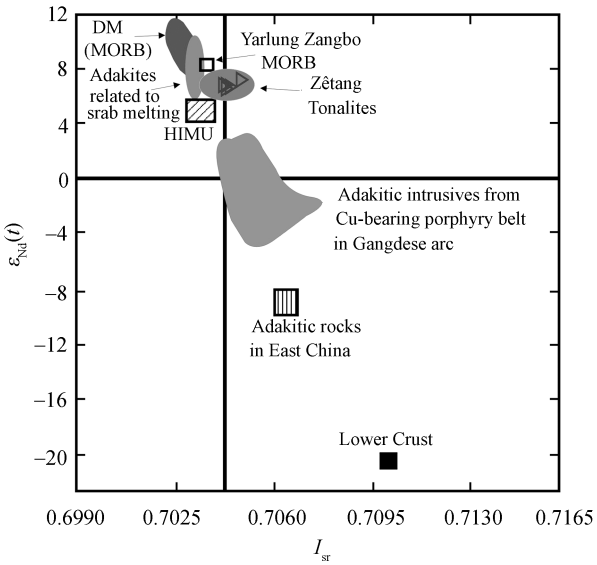

Figure 7 $\varepsilon_{Nd}(t)$-I_{Sr} diagram[14].

three ways: (1) AFC process[35]; (2) melting of subducted oceanic crust[1,36]; and (3) underplating basalt/delaminated lower crustal melting[2]. Geochemical characteristics and geological background of Zêtang tonalites suggest that these rocks should be generated by slab melting rather than the other origins. Our proposal is supported by the following evidence:

(1) There are no large volumes of mafic rocks occuring in the studied area and Zêtang tonalites do not exhibit a fractionation trend in the Harker diagrams. These clues suggest that the tonalites are unlikely generated through AFC process.

(2) The adakites, derived from underplating basalt/delaminated lower crustal melting, are the products of vertical growth of continental crust. In the thickened crust (>40 km), both the partial melting of lower crustal basaltic materials and delaminated crustal melting can produce the rocks with adakitic geochemical signatures, such as the adakites in Andes[37], Eastern China[6,38−40] or Northern Tibet[7−11]. Adakites produced by the lower crustal melting show obvious crustal characteristics in isotope (high Sr and low Nd). I_{Sr} values of the volcanic rocks originated from lower crust, generally range between 0.706−0.710[9] and I_{Nd}<0.5126[2]. Zêtang tonalites have relatively low I_{Sr} (0.70421−0.70487), high $^{143}Nd/^{144}Nd$ (0.512896−0.512929) and $\varepsilon_{Nd}(t)$ values (+6.7−+7.3). This suggests that Zêtang tonalites originated from depleted mantle rather than the continent crustal melting. In addition, Zêtang tonalites crop out in the Yarlung Zangbo suture zone which represents the

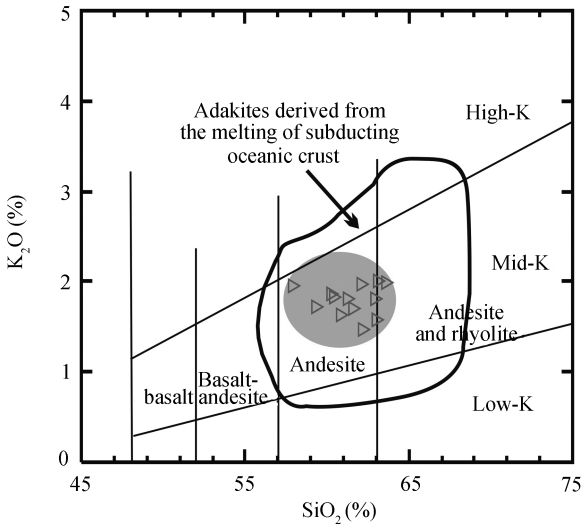

Figure 8 SiO_2-K_2O diagram[1,42]

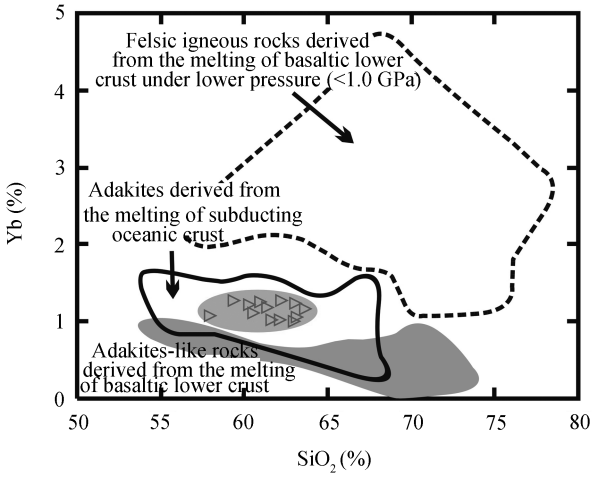

Figure 9 SiO_2-Yb diagram[43].

remnants of Tethys ocean between India and Asia continents. Their outcrop environment is similar to that of the modern suducted-type adakites around the Pacific, obviously different from the continental within-plate setting such as Eastern China and Northern Tibet. Hence, the possibility that Zêtang tonalites were formed by the melting of under-plating basalt/delaminated lower crust can be precluded.

(3) The source rocks of subducted-type adakites are the oceanic crust with MORB features, hence its isotope compositions must be characterized by MORB (I_{Nd}> 0.5130, I_{Sr}<0.7040). Zêtang tonalites have similar isotopic features with MORB and are close to the field of the adakites originated by sudubcted oceanic crust with small volume involvement of oceanic sediments (I_{Nd} = 0.5125, I_{Sr}=0.7050)[41]. These evidences support the proposal that Zêtang tonalites were derived from the partial melting of oceanic crust with MORB characteristics.

(4) The subducted-type adakites generally interact with mantle wedge in the ascending process, which would result in the increases of MgO, Cr, Ni contents. Cr and Ni contents of Zêtang tonalites (on average 94×10^{-6} and 52×10^{-6}) are obviously higher than those in the typical adakites (on average 46×10^{-6} and 24×10^{-6})[42], indicating the interaction between melt and mantle wedge. The low MgO content of samples should be noticed, which is similar to that of the subducted-type Xiwan albite granites[32] but lower than the Cenozoic adakites in Northern Tibet that formed by lower crustal melting[7]. As shown by the SiO_2-K_2O (Figure 8) and SiO_2-Yb (Figure 9) diagrams, the samples are all plotted in the field of the adakites derived from the melting of subducting oceanic crust, but far from the adakites derived from the melting of basaltic lower crust. In Cr-Ni diagram (Figure 10), all samples extend along the partial melting line of eclogite and are distributed around the mixed zone of mantle components and MORB.

(5) The adakites derived from slab melting usually coexist with island arc and SSZ-type ophiolite. As a part of the Yarlung Zangbo suture zone, Zêtang tonalites were exposed within the Zêtang island arc rock assemblage and cropped out accompanying with the SSZ-type Zêtang ophiolite. This geological evidence also suggests that they were closely related to the subduction.

(6) Zêtang tonalites are abundant in tourmaline and apatite, which are rich in volatile components (e.g. H_2O, B, P, etc.). Ishikawa & Nakamura[45] pointed out that B-Be and B-Nb never fractionate between minerals and melt in the partial melting process whereas they strongly fractionate in fluid and B resides in the fluid. The ubiquitous tourmaline in Zêtang tonalites suggests B enrichment in the rocks, implying the addition of subducted components during the melting process.

(7) Zêtang tonalites are significantly depleted in Nb, Ta and Ti. The causes resulting in the depletion can be summarized as follows[46]: (1) Crystal fractionation of Fe-Ti oxides in the crust; (2) fractionation of Ti-rich, hydrous silicates such as phlogopite of hornblende in the

mantle or crust; (3) extensive, chromatographic interaction between migrating melt and depleted peridotite; (4) the presence of phases such as rutile or sphene in the mantle wedge; (5) relative immobility of Ta and Nb relative to REE and other elements in aqueous fluids derived from subducting material; (6) inherited, low Ta/Th and Nb/Th from subducted sediment; and (7) the presence of residual rutile during partial melting of subducted material. Amphibole and biotite are prevailing in Zêtang tonalites while little pyroxene and Ti-Fe oxides can be found. Hence, the depletion of Nb, Ta and Ti should be related to (3)－(7) processes, that is to say, the interaction between subducted components and depleted mantle.

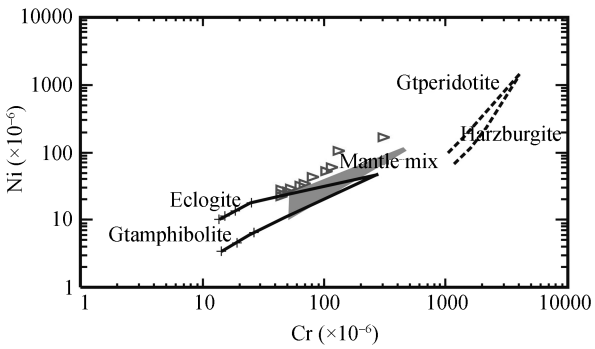

Figure 10 Cr-Ni diagram[44]. The real line represents partial melting curve of MORB; the residue is 10% garnet amphibolite and eclogite; the dash lines represent partial melting lines of garnet peridotite and harzburgite. The cross symbols represent melting percentage: from left to right, it is 1%, 10%, 30%, 50%, respectively; the shadow represents the zone of 1%－10% mantle components mixed into 1%－50% MORB.

(8) Zêtang tonalites are obviously depleted in HREE and Y, indicating that garnet is an important residual mineral. But their Sr/Y and La/Yb ratios are not so high compared with those of typical adakites, and shows a little higher than those of the island arc volcanic rocks. In Zêtang tonalities, MREE is more depleted than HREE, implying that garnet is not the only residual mineral to control the compositions.

Zêtang tonalites are enriched in Sr, Al and show faint Eu positive anomaly, suggesting that plagioclase was unstable in residue and had entered the melt. When the residue is mainly composed of garnet, the melt is characterized by significant depletion in HREE ($Y/Yb>10$, $(Ho/Yb)_N>1.2$). However, when the amphibole dominates in the residue, HREE generally exhibits a flat pattern ($Y/Yb\approx10$, $(Ho/Yb)_N\approx1$)[47]. For Zêtang tonalites, the ratios of Y/Yb and $(Ho/Yb)_N$ are 7.8－8.9 (on average 8.4) and 0.77－0.86 (on average 0.8), respectively, and MREE are more depleted than HREE. These geochemical features show that amphibole should be the primary residual facies. As shown by the Sr/Y-Y diagram (Figure 5), samples are plotted between garnet amphibolite and amphibole eclogite lines. In the $(La/Yb)_N$-Yb_N diagram (Figure 6), samples also are located around the partial melting line of 10% garnet amphibolite. Accordingly, it can be inferred that the source residue facies were mainly composed of amphibole and garnet, probably, with a small amount of clinopyroxene. The proportion of amphibole in the residue is slightly higher than in the typical adakites whereas the proportion of garnet is relatively low. Because of strong HREE enrichment in garnet and MREE enrichment in amphibole, the residue facies component (Amphibole+Garnet+Clinopyroxene) results in an obvious depletion of MREE than HREE in Zêtang tonalites, accompanied by the increase of Y and Yb contents and the decreases of Sr/Y and La/Yb ratios. This is consistent with the experimental results. The results of experimental petrology show that[36,48], under certain temperature and pressure conditions, the dehydrated melting of subducted oceanic crust (partial melting of amphibole) can produce the adakitic melt, and the residue facies are granet+clinopyroxene+amphibole, similar to the situation discussed in this paper.

According to the above discussion, it can be concluded that Zêtang tonalites were produced by the partial melting of young and hot subducted oceanic crust in certain depth (amphibolite-eclogite transition zone), and the residue may be composed of amphibole+garnet+clinopyroxene. During the melting process, small volume of oceanic sediments were involved into the melt, resulting in a slight change of the composition. Furthermore, the melt interacted with the peridodite in small proportion when migrating through the mantle wedge.

4.2 Geodynamic significance

The adakites derived from slab melting reveal the deep partial melting process of young (＜25 Ma) and hot oceanic crust subducting at a low angle. The melting depth approximated 75－85 km (corresponding to amphibolite-eclogite transition zone), obviously less than the formation depth of island arc volcanic magma (120－150 km)[49]. This type of adakite was produced in the early subduction, and was closer to the trench than

island arc volcanic rock. Thus, the direction from adakite to normal island arc volcanic rock suggests the subduction direction of oceanic slab. Therefore, the occurrence of subducted-type adakites marks the beginning of the oceanic crust subduction, and probably implies that the ocean starts to shrink[50,51].

The Yarlung Zangbo suture zone represents the Tethys oceanic remnants after Indian-Asian continent collision and Tethyan extinction. For the tectonic models of Indian-Asian continent collision, the most widely accepted one is that the Tethys oceanic crust subducted along the south margin of Lhasa terrane, and ultimately led to the Indian-Asian continent collision and the Tibetan Plateau uplift[52,53]. But recent work shows that this model may be too simple and the evolution of Tethys ocean is more complicated. Allegre et al.[54] suggested the existence of intra-oceanic island arc in Tethys, which probably had completely disappeared. Searle et al.[52] also suggested that the most important difference between Tibet and western Himalaya was the absence of evidence to prove the previous existence of an intra-oceanic island arc in Tibet. Actually, in the Kohistan and Ladakh areas within the western Yarlung Zangbo suture zone, a suit of Kohistan-Dras intra-oceanic island arc rocks have been identified and were thought to be the products of intra-Tethyan oceanic subduction[55,56]. Here, very interesting questions arise —— whether there was intra-oceanic island arc in the eastern Yarlung Zangbo suture zone? If yes, what is the relation between this arc and the Kohistan-Dras intra-oceanic arc? These questions are very important for well understanding the Tethyan tectonic evolution and the Indian-Asian collision process. Based on the detailed field investigations in the Zêtang segment of the Yarlung Zangbo suture zone, Aichison et al.[22,23] suggested the existence of a Mesozoic intra-oceanic subduction system. They identified Zêtang terrane, Dazhuqu terrane and Bainang tersenting intra-oceanic island arc, forearc ophiolite (namely Zêtang ophiolite) and subduction complex, respectively. Furthermore, they also suggested that Tethys ocean began to subduct and consume here. This model is mainly based on the field geological investigations and some palaeontological evidence, but lack of more geochemical evidence.

Our identification of subducted-type adakites in the Zêtang area within the eastern Yarlung Zangbo suture zone suggests the existence of an intra-oceanic subduction belt. The island arc rock assemblage in the north of Zêtang ophiolite represents the intra-oceanic island arc (Zêtang island arc) formed above the subduction belt and the product of early northward subduction of Tethys oceanic lithosphere. According to the published geochronological data of Zêtang island arc (152－161 Ma[24]), we can approximately constrain the commenced time of this intra-oceanic subduction event in Mid-Late Jurassic.

These new evidence and insights give the supports for the existence of intra-oceanic island arc within Tethys ocean and are helpful to better understanding the formation and evolution in Zêtang segment of the Yarlung Zangbo suture zone.

5 Conclusions

Zêtang tonalites exposed within the Zêtang island arc rock assemblage of the eastern Yarlung Zangbo suture zone display the adakitic geochemical features and were produced by the partial melting of subducted oceanic crust. The identification of Zêtang subducted-type adakites suggests the existence of subduction belt and intra-oceanic island arc within Tethys ocean. Based on the previous data and geological background, it can be inferred that this subduction event commenced in Mid-Late Jurassic.

The authors would like to thank Dr. He Hongping from Guangzhou Insititute of Geochemistry for helping to amend the English manuscript. We are also grateful to two anonymous referees and the editors for the precious advice.

1 Defant M J, Drummond M S. Derivation of some modern arc magmas by melting of young subducted lithosphere. Nature, 1990, 347: 662－665
2 Atherton M P, Petford N. Generation of sodium-rich magmas from newly underplated basaltic crust. Nature, 1993, 362: 144－146
3 Kay S M, Coira B, Viramonte J. Young mafic back-arc volcanic rocks as guides to lithospheric delamination beneath the Argentine Puns Plateau, Central Andes. J Geophys Res, 1994, 99: 14323－14339
4 Kay S M, Ramos V A, Marquez Y M. Evidence in Cerro Pampa volcanic rocks for slab-melting prior to ridge-trench collision in southern South America. J Geol, 1993, 101: 703－714
5 Zhang Q, Wang Y, Qian Q, et al. The characteristics and tectonic-metallogenic significances of the adakites in Yanshan period from eastern China. Acta Petrol Sin (in Chinese), 2001, 17(2): 236－244
6 Zhang Q, Qian Q, Wang E Q, et al. An east China plateau in mid-late

Yanshanian period: implication from adakites. Chin J Geol (in Chinese), 2001, 36(2): 129－143
7 Lai S C. Identification of the Cenozoic adakitic rock association from Tibetan plateau and its tectonic significance. Earth Sci Front (in Chinese), 2003, 10(4): 407－415
8 Xu J F, Wang Q. Tracing the thickening process of continental crust through studying adakitic rocks: evidence from volcanic rocks in the north Tibet. Earth Sci Front (in Chinese), 2003, 10(4): 401－406
9 Wei J Q, Yao H Z, Niu Z J, et al. Identification of the adakitic rock association in Chibzhang Co area, northern Tibet, and its significance. Acta Petrol Mineral (in Chinese), 2005, 24(3): 173－178
10 Chung S L, Liu D Y, Ji J Q, et al. Adakites from continental collision zone: Melting of thicken lower-crust beneath southern Tibet. Geology, 2003, 31: 1021－1024
11 Wang Q, McDermott F, Xu J F, et al. Cenozoic K-rich adakitic volcanic rocks in the Hohxil area, northern Tibet: Lower-crustal melting in an intracontinental setting. Geology, 2005, 33: 465－468
12 Hou Z Q, Meng X J, Qu X M, et al. Copper ore potential of adakitic intrusives in Gangdese porphyry copper belt: Constrains from rock phase and deep melting process. Miner Deposits (in Chinese), 2005, 24(2): 108－121
13 Gao Y F, Hou Z Q, Wei R H. Neogene porphyries from Gangdese: petrological, geochemical characteristics and geodynamic sighificances. Acta Petrol Sin (in Chinese), 2003, 19(3): 418－428
14 Hou Z Q, Gao Y F, Qu X M, et al. Origin of adakitic intrusives generated during mid-Miocene east-west extension in South Tibet. Earth Planet Sci Lett, 2004, 220: 139－155
15 Hou Z Q, Gao Y F, Meng X J, et al. Genesis of adakitic porphyry and tectonic controls on the Gangdese Miocene porphyry copper belt in the Tibetan orogen. Acta Petrol Sin (in Chinese), 2004, 20(2): 239－248
16 Qu X M, Hou Z Q, Guo L J, et al. Source compositons and crustal contaminations of adakitic orc-bearing porphyries in the Gangdise copper belt: Nd, Sr, Pb and O isotope constraints. Acta Geol Sin (in Chinese), 2004, 78(6): 813－821
17 The Qinghai-Tibetan Plateau Science Expedition of the Chinese Academy of Sciences. Magmatism and Metamorphism in Xizang (Tibet) (in Chinese). Beijing: Science Press, 1981. 1－50
18 Bureau of Geology and Mineral Resources of Tibet Autonomous Region. Regional Geology of Xizang (Tibet) Autonomous Region (in Chinese). Beijing: Geological Publishing House, 1993. 170－300
19 Xia B, Guo L Z, Shi Y S. The Zêtang ophiolite of Tibet and its plate tectonics significance. J Nanjing University (Earth Sci) (in Chinese), 1989, 3: 19－29
20 Gao H X, Song Z J. New progress in the study of the Zêtang ophiolitic melange in Tibet. Reg Geol China (in Chinese), 1995, 4: 316－322
21 Wei D L, Xia B, Zhou G Q, et al. The lithochemistry characteristics and origin of the Zêtang ophiolite crust volcanic lava in Xizang (Tibet), China. Geotec Metal (in Chinese), 2004, 28(3): 270－278
22 Aitchison J C, Badengzhu, Davis A M, et al. Remnants of a Cretaceous intra-oceanic subduction system within the Yarlung-Zangbo suture (southern Tibet). Earth Planet Sci Lett, 2000, 183: 231－244
23 Aitchison J C, Davis A M, Abrajevitch A V, et al. Stratigraphic and sedimentological constraints on the age and tectonic evolution of the Neotethyan ophiolites along the Yarlung Tsangpo suture zone, Tibet. In: Dilek Y, Robinson P T, eds. Ophiolites in Earth History. London: The Geological Society, 2003. 147－164
24 McDermid I R C, Aitchison J C, Davis A M, et al. The Zêtang terrane: a Late Jurassic intra-oceanic magmatic arc within the Yarlung-Tsangpo suture zone, southeastern Tibet. Chem Geol, 2002, 187: 267－277
25 Mcdermid I R C. Zêtang terrane, south Tibet. Dissertation for the Doctoral Degree. Hongkong: Hongkong University, 2003. 19－20
26 Qi L, Hu J, Gregoire D C. Determination of trace elements in granites by inductively coupled plasma mass spectrometry. Talanta, 2000, 51: 507－513
27 Chen F, Siebel W, Satir M, et al. Geochronology of the Karadere basement (NW Turkey) and implications for the geological evolution of the Istanbul zone. Int J Earth Sci, 2002, 91: 469－481
28 Chen F, Hegner E, Todt W. Zircon ages, Nd isotopic and chemical compositions of orthogneisses from the Black Forest, Germany: evidence for a Cambrian magmatic arc. Int J Earth Sci, 2000, 88: 791－802
29 Barker F. Trondhjemite: definition, environment and hypotheses of origin. In: Barker F, ed. Trondhjemites, Dacites and Related Rocks. Amsterdam: Elsevier, 1979. 1－12
30 Defant M J, Jackson T E, Drummond M S, et al. The geochemistry of young volcanism throughout western Panama and southeastern Costa Rica: an overview. J Geol Soc London, 1992, 149: 569－579
31 Zhang H X, Niu H C, Hiroaki S, et al. Late Paleozoic adakite and Nb-enriched basalt from northern Xinjiang: evidence for the southward subduction of the Paleo-Asian ocean. Geol J Chin Universities (in Chinese), 2004, 10(1): 106－113
32 Li W X, Li X H. Adakitic granites within the NE Jiangxi ophiolites, South China: geochemical and Nd isotopic evidence. Precambrian Res, 2003, 122: 29－44
33 Drummond M S, Defant M J. A model for trondhjemite-tonalite-dacite genesis and crustal growth via slab melting: Archaean to modern comparisons. J Geophys Res, 1990, 95: 21503－21521
34 Martin H. Effect of steeper Archaean geothermal gradient on geochemistry of subduction-zone magmas. Geology, 1986, 14: 753－756
35 Castillo R P, Janney P E, Solidum R S. Petrology and geochemistry of Camiguia Island, Southern Philippines: insight to the source of adakites and other lavas in a complex arc setting. Contrib Miner Petrol, 1999, 134: 33－51
36 Peacock S M, Rushmer T, Thompson A B. Partial melting of subducting oceanic crust. Earth Planet Sci Lett, 1994, 121: 227－244
37 Kay R W, Kay S M. Creation and destruction of lower continental crust. Geologiche Rundschau, 1991, 80: 259－278
38 Wang Q, Zhao Z H, Xiong X L, et al. Melting of the underplated basaltic lower crust: evidence from the Shaxi adakitic sodic quartz diorite-porphyrites, Anhui Province, China. Geochimica (in Chinese), 2001, 30(4): 353－362
39 Xu J F, Wang Q, Xu Y G, et al. Geochemistry of Anjishan intermediate-acid intrusive rocks in Ningzhen area: Constraint to origin of the magma with HREE and Y depletion. Acta Petrol Sin (in Chinese), 2001, 17(4): 576－584
40 Xu J F, Shinjo R, Defant M J, et al. Origin of Mesozoic adakitic intrusive rocks in the Ningzhen area of east China: partial melting of delaminated lower continental crust? Geology, 2002, 30: 1111－1114

41 Stern C R, Kilian R. Role of the subducter slab, mantle wedge and continental crust in the generation of adakites from the Austral Volcanic Zone. Contrib Miner Petrol, 1996, 123: 263－281
42 Martin H. Adakitic magmas: modern analogues of Archean granitoids. Lithos, 1999, 46: 411－429
43 Wang Q, Zhao Z H, Xu J F, et al. Petrogenesis and metallogenesis of the Yanshanian adakite-like rocks in the Eastern Yangtze Block. Sci China Ser D-Earth Sci (in Chinese), 2002, 32(Suppl.): 127－136.
44 Luo Z H, Ke S, Kan H W. Characteristics, petrogenesis and tectonic implications of adakite. Geol Bull Chin (in Chinese), 2002, 21(7): 430－440
45 Ishikawa T, Nakamura. Origin of the slab component in arc lavas from across-arc variation of B and Pb isotopes. Nature, 1994, 370: 205－208
46 Kelemen P B, Hanghøj K, Greene A R. One view of the geochemistry of subduction-related Magmatic Arcs, with an emphasis on primitive andesite and lower crust. In: Rudnick R L, ed. The Crust, Treatise on Geochem. Amsterdam: Elsevier, 2003. 593－659
47 Ge X Y, Li X H, Chen Z G, et al. Geochemistry and petrogenesis of Jurassic high Sr/low Y granitoids in eastern China: constraints on crustal thickness. Chin Sci Bull, 2002, 47(11): 962－968
48 Xu H J, Ma C Q. Constraints of experimental petrology on the origin of adakites, and petrogenesis of Mesozoic K-rich and high Sr/Y ratio granitoids in eastern China. Earth Sci Front (in Chinese), 2003, 10(4): 417－427
49 Crosson R S, Owens T J. Slab geometry of the Casca-dia subduction zone beneath Washington from earth-quake hypocenters and teleseismic converted waves. Geophys Res Lett, 1987, 14: 824－827
50 Sajona F G, Mury R C, Bellon H, et al. Initiation of subduction and the generation of slab melts in western and eastern Mindanao, Philippines. Geology, 1993, 21: 1007－1010
51 Zhu D C, Pan G T, Duan L P, et al. Some problems in the research of adakite. NW Geol (in Chinese), 2003, 36(2): 13－19
52 Searle M P, Windley B F, Coward M P, et al. The closing of Tethys and the tectonics of the Himalaya. Geol Soc Am Bull, 1987, 98: 678－701
53 Durr S B. Provenance of Xigaze fore-arc basin clastic rock (Cretaceous, South Tibet). Geol Soc Am Bull, 1996, 108: 669－684
54 Allegre C J, Courtillot V, Tapponnier P, et al. Structure and evolution of the Himalaya-Tibet orogenic belt. Nature, 1984, 307: 17－22
55 Robertson A H, Degnan P. The Dras arc complex: lithofacies and reconstruction of a Late Cretaceous oceanic volcanic arc in the Indus suture zone, Ladakh Himalaya. Sed Geol, 1994, 92: 117－145
56 Searle M P, Khan M A, Fraser J E, et al. The tectonic evolution of the Kohistan-Karakoram collision belt along the Karakoram Highway transect, north Pakistan. Tectonics, 1999, 18: 929－949